Economics of Using Additive Manufacturing to Fabricate a Molten Salt-to-Supercritial Carbon Dioxide Heat Exchanger for Concentrating Solar Power

Tracey Ziev[a,e], Erfan Rasouli[b], Ines-Noelly Tano[b], Ziheng Wu[c], Srujana Rao Yarasi[c], Nicholas Lamprinakos[c], Junwon Seo[c], Vinod Narayanan[b], Anthony D. Rollett[c], Parth Vaishnav[d,a]

[a]*Department of Engineering and Public Policy, Carnegie Mellon University, 5000 Forbes Avenue, Pittsburgh, 15213, PA, USA*
[b]*Department of Mechanical and Aerospace Engineering, University of California, Davis, One Shields Avenue, Davis, 95616, CA, USA*
[c]*Department of Materials Science and Engineering, Carnegie Mellon University, 5000 Forbes Avenue, Pittsburgh, 15213, PA, USA*
[d]*School for Environment and Sustainability, University of Michigan, 440 Church Street, Ann Arbor, 48109, MI, USA*
[e]*Corresponding author: tlz@andrew.cmu.edu,*

Abstract

Advances in manufacturing technologies and materials are crucial to the commercial deployment of energy technologies. We present the case of concentrating solar power (CSP) with molten salt thermal storage, where low cost, high efficiency heat exchangers (HX) are needed to achieve cost-competitiveness. The materials required to tolerate the extreme operating conditions in CSP systems make it difficult or infeasible to produce them using conventional manufacturing processes. While it is technically possible to produce HXs with adequate performance using additive manufacturing, specifically laser powder bed fusion (LPBF), here we assess whether doing so is cost-effective. We describe a process-based cost model (PBCM) to estimate the cost of fabricating a molten salt-to-supercritical carbon dioxide HX using LPBF. The PBCM is designed to identify modifications to designs, process choices, and manufacturing innovations that have the greatest effect on manufacturing cost. Our PBCM identified HX design and LPBF process modifications that reduced projected HX cost from $780 per kilo-Watt thermal (kW-th) to $570/kW-th using currently available LPBF technology, and down to $270/kW-th with improvements in LPBF technology that are likely to be

achieved in the near term. The PBCM also informed a redesign of the HX design that reduced projected costs to $130-170/kW-th.

Keywords: additive manufacturing, techno-economic modeling, pin fin heat exchanger, concentrating solar power, molten salt-to-supercritial carbon dioxide

---

1. Introduction

Advancing clean energy technologies requires innovations in manufacturing to enable cost effective productions of high performance systems and components. Further, it is necessary to minimize impacts that manufacturing clean energy technologies has on the environment. [1] Additive manufacturing (AM) is a promising option to address manufacturing challenges presented by clean energy technology. One such potential application is the primary heat exchanger (HX) for concentrating solar power (CSP) systems with molten salt (MS) thermal energy storage.

CSP with thermal energy storage is an attractive technology because it inherently addresses grid integration challenges presented by other clean energy technologies such as wind and solar photovoltaics due to its energy storage capacity. However, efficiency improvements and cost reductions are needed for CSP to be cost competitive with other forms of electricity generation.[2]

In order to achieve the desired thermal-electric cycle efficiency ($\geq 50\%$), CSP requires a high-temperature power cycle, such as a Brayton supercritical carbon dioxide cycle (sCO_2). This cycle presents demanding operating conditions: ≥ 700°C hot-side temperature and ≥ 20 MPa operating pressure. [2] Currently, HX account for 60 - 70% of sCO_2 Brayton cycle powerblock cost, so reduction in cost of the HX are necessary for CSP to be cost-competitive. [3]

Currently, the baseline technology for fabricating a high efficiency HX is a diffusion bonding based microlamination process. In microlamination, the HX is fabricated by photochemically etching a channel pattern onto thin metal shims, stacking the shims, diffusion bonding under high temperature and pressure, and welding traditionally manufactured inlet and outlet headers to the diffusion bonded core. [4] Investigations of diffusion bonding with high temperature alloys have shown that defects form in the bond region that reduce the creep and fatigue life of the bonded material as compared to the material's sheet form. [5, 6] In addition to the technical challenge of dif-

fusion bonding high temperature resistant alloys, microlamination produces relatively expensive HXs. This requires alternative manufacturing processes to reduce primary HX cost. [2]

Additive manufacturing (AM) holds promise as an alternative technique for manufacturing a high efficiency HX. Since AM enables manufacturing of complex parts with intricate geometries, including internal passages, that would be difficult or impossible to fabricate via traditional manufacturing processes, it unlocks design flexibility to increase the energetic and volumetric efficiency of HXs. Additionally, AM enables use of materials that retain high strength at elevated temperatures and are resistant to chemical attack. [7] AM HXs incorporate microscale heat transfer features to increase HX efficiency while maintaining or decreasing HX size [8]. Laser Powder Bed Fusion (LPBF), a form of AM where a laser melts powdered material to form each layer of the part, has been successfully used to demonstrate fabrication of AM HX designs for aerospace and power generation applications [8, 9, 10, 11, 12]. These investigations of using AM for HX design focus primarily on design for HX performance, with limited consideration of manufacturing cost. Given the importance of cost to CSP adoption, we evaluate cost along with the HX performance and LPBF process parameter selection.

We use Process Based Cost Modeling (PBCM) to evaluate the cost of manufacturing a LPBF-fabricated HX for use as the molten salt (MS)-to-(sCO_2) primary HX for CSP systems. We chose PBCM because it enables us to integrate cost into the part and manufacturing process design process. [13] PBCM builds the total part cost from the costs associated with each step of the manufacturing process. The cost for each process step is modeled from the contributing components (e.g. capital, material, labor, etc.) and their relationship to the part's design (e.g. dimensions, material choice, etc.), processing parameters (e.g. cycle time, heating/cooling time, etc), and facility operating parameters (e.g. operating hours, production volume, etc.). [14] PBCM has been used to estimate costs for a variety of applications including automotive, aerospace, and energy storage. [15, 16, 17, 18] PBCM can also be used in conjunction with other models to simultaneously design for multiple objectives. [19, 20] Cost models for the production of microchannel HX exist, but these models are typically developed post-hoc. [21, 22, 23] We integrate our PBCM with the HX performance model and use it as a tool to enable an iterative design process for the HX design and LPBF process parameter selection. Our PBCM estimates the cost of a four-step manufacturing process consisting of 3D printing via LPBF, heat treatment to relieve residual

stresses, removing the HX from the support structures and base with a computer numerically controlled (CNC) band saw, and internal passage cleaning and smoothing via abrasive flow machining (AFM) which forces an abrasive polymer through the part to smooth the surfaces.

2. Heat Exchanger and Manufacturing Process Design

To evaluate the potential for use of a AM-fabricated heat exchanger for solar thermal applications, we designed a small-scale MS-to-sCO_2 HX (Figure 1) to meet the same performance requirements as the larger scale HX, with the exception of the heat transfer rating (in kW-th). The MS enters at nominal pressure of 1 bar and temperature of 720 °C. The sCO_2 enters the HX at nominal pressure of 200 bar and temperature of 500 °C. Haynes 282, a nickle superalloy, is chosen as the material for the HX due to its high creep strength at the design temperatures [24].

We considered sCO_2 pressure drop, drainage of MS, thermal and flow characteristics, thermal stresses, creep, and fatigue in designing the HX. First, we designed a repeating unit cell of the pin array that could withstand 200 bar pressure. We determined bounding pin array dimensions to ensure the HX core did not experience ¿100 MPa stress (based on rupture strength of H282 for 100,000 hours of operation). We then developed a thermofluidic model to determine the dimensions of the HX to maximize effectiveness and power density. Next, we designed the sCO_2 headers for mechanical strength and to ensure uniform flow distribution (Figure 1). We performed a conjugate computational fluid dynamics simulation on a pair of hot and cold channels to determine the thermal stresses. We then performed creep simulations, based on the Norton model, on the core and header regions to determine whether the HX could operate for 100,000 hours at the design temperature and pressure for continuous and cyclic operation [25].

The HX consists of a series of spaced plates connected via sCO_2 inlet and outlet headers. MS flows around and between the plates. The core of the HX consists of repeating pin array sCO_2 channels and finned MS channels. The sCO_2 side pin array has transverse pin spacing, S_T, of 2.46 mm, longitudinal spacing, S_L, of 2.13 mm, pin diameter, D_pin, of 1.2 mm, and channel width, W_C, of 1.8 mm. Additional structures are added at the inlet and exit locations to improve flow distribution and maintain structural integrity. The MS finned side has channel width, W_H, of 1 mm and fin spacing distance S_{fin} of 5 mm apart. The plates are length, l_p, of 240 mm,

width, w_p, of 100 mm, and height, h_p, of 50 mm. The dimensions of each of the two headers are length, l_h, of 60 mm, width, w_h, of 160 mm, and height, h_h, of 60 mm. Multiple such HX can be combined using common headers to form a multi-MW scale HX for the primary MS-to-sCO_2 HX for CSP.

We evaluate production of the small-scale HX design via LPBF in an EOS M290 single 400 W laser machine. [26] The key parameters controlling the LPBF process are laser power, P, laser scan speed, v, hatch spacing (distance between laser scan passes), H, and layer thickness, L. The LPBF processing parameters impact the time required for 3D printing; build rate for the part is approximately proportional to vHL. Increasing v, H, and/or L will increase the build rate which reduces build cycle time and in turn reduces cost. The LPBF processing parameters also impact the defect content of the part, which has been shown to degrade fatigue life of AM parts [27, 28]. Porosity defects in LPBF are correlated with energy density, E, which is approximately proportional to $\frac{P}{vHL}$ [29]. At low E, lack of fusion porosity occurs due to incomplete melting of the powder. At high E, keyhole porosity occurs due to instability in the meltpool. At combinations of high P and v, bead-up occurs causing porosity and/or contact with the the powder recoater blade. [30, 31, 32] We can select processing parameters for LPBF from within the region bounded by these three porosity defect regimes. For our baseline cost estimate, we conservatively use process parameters that produced the lowest porosity during parameter set testing in Haynes 282. Our baseline parameter set uses P 370 W, v 700 mm/s, H 110 microns, and L 40 microns.

To evaluate the feasibility of the 3D printing the design and configuration of the pin arrays in the sCO_2 channel, we 3D printed single channel HX testing units. We used these testing units to evaluate printability, test post-processing depowdering and heat treatments, and perform heat transfer and pressure drop testing (Figure 1).

3. Methods

3.1. Process Based Cost Modeling

Our PBCM models HX total cost as a sum of the costs for each manufacturing process step and material cost, c_{mat} (Equation 1). The cost for each process step is modeled as a function of equipment cost, c_{equip}, labor cost, c_{labor}, facility cost c_{fac}, consumables cost, c_{cons}, utility cost, c_{util}, and overhead cost, c_{over}. As described below and more extensively in the supplemental materials, we collected input data for our baseline model from

multiple sources including existing literature, trade and vendor publications and websites, vendor quotes, and discussions with AM experts.

$$c_{unit} = c_{mat} + c_{eq} + c_{lab} + c_{fac} + c_{cons} + c_{util} + c_{over} \quad (1)$$

To account for uncertainty in the cost estimate, we conduct a Monte Carlo simulation, varying key input parameters for 3D printing costs. These parameters include material price, machine price, machine life, cycle labor fraction, scrap rate, part acceptance rate, manufacturing technician salary, and electricity cost. The ranges we use for these values are noted in the rest of the methods section. We assume that the values of these parameters are uniformly distributed between these ranges. For each iteration of the Monte Carlo simulation, we sample values from this distribution. For each calculation where uncertainty is represented, we conduct 1,000 iterations of the Monte Carlo simulation, and calculate the mean and standard deviation of the samples. We report two standard deviations as the uncertainty range for the cost estimates.

3.1.1. Annual and Effective Production Volumes

We specify the number of HXs to be produced each year, the annual production volume (APV). We use APV 1,500 units, the approximate number required for a single 20 MW CSP plant. To account for defective parts, we calculate an effective production volume, EPV, required to produce the APV of saleable units. We calculate EPV as a function of APV and the product of the part acceptance rates, y_{ps}, for each of n_{ps} process steps (Equation 2). We use EPV as the quantity input to calculate total cost for each cost category then divide by APV to distribute costs across the saleable units. We assume y_{ps} 80-95% for LPBF, 100% for heat treating, 98% for removing supports/base plate, and 99% for AFM per Carnegie Mellon University (CMU) NextManufacturing and equipment vendors.

$$EPV = \frac{APV}{\prod_{i=1}^{n_{ps}} y_i} \quad (2)$$

3.1.2. Material Cost

We calculate material cost per unit, c_{mat}, as a function of HX mass, m, scrap rate, r_s, and material price, p_{mat} (Equation 3). For H282, we use a range of \$125-145/kg based on the vendor-quoted price of \$139/kg.

We assume r_s to be 5-15% based on the 10% recommendation from CMU NextManufacturing [33].

$$c_{mat} = p_{mat} m (1 + r_s) \tag{3}$$

3.1.3. Equipment Cost

For each process step, we calculate annual cost of equipment as a function of machine price, p_{mch}, an equipment capital recovery factor, CRF, installation price, p_{inst}, annual maintenance cost, p_{mnt}, and number of machines required to produce EPV units, n_{mch} (Equation 4).

$$c_{eq} = \frac{n_{mch}(CRF p_{mch} + p_{inst} + p_{maint})}{APV} \tag{4}$$

We use p_{mch} \$535,000-700,000 for LPBF [34], \$50k for heat treating [16], \$65k for removing supports/base plate [35], and \$170k for AFM (vendor quote). We calculate CRF as a function of discount rate, d, and expected machine life, $t_m l$ (Equation 5). We use the average US small business discount rate of 8.5% [36] for d. For t_{ml}, we use the average 3D printer life of 7-10 yrs for LPBF [37], and for all other process steps assume t_{ml} 20 yrs.

$$CRF = \frac{d(1 + d)^t_{ml}}{(1 + d)^t_{ml} - 1} \tag{5}$$

For p_{inst}, we use \$47k for LPBF [34], and for all other process steps assume p_{inst} is 10% of p_{mch}. For c_{mnt}, we use \$58k for LBPF [34], and for all other process steps assume p_{mnt} is 5% of p_{mch} per year. We calculate n_{mch} as a function of EPV, annual machine operating hours, t_{op}, machine set-up/teardown time (including heat-up/cooldown time), t_{st}, and cycle time, t_{cyc} (Equation 6). We assume t_{op} 8064 hrs (92% up time). We assume t_{st} 9.5 hrs for LPBF, 8hrs for heat treating, 0.5 hrs for removing supports/base plate, and 0.5 hrs for AFM per CMU NextManufacturing and equipment vendors. We used t_{cyc} 135 hrs $+/-10\%$ for LPBF (see Section 3.1.4), 4 hrs for heat treating, 6 hrs for removing supports/base plate, and 1 hr for AFM per CMU NextManufacturing and equipment vendors.

$$n_{mch} = \frac{EPV(t_{st} + t_{cyc})}{t_{op}} \tag{6}$$

3.1.4. HX Build Cycle Time

We divide our build cycle time calculation into two parts, raster time, t_r, and powder spread time, t_{ps}. To calculate t_r, we divide the HX into segments that can be approximated as having a constant cross-section. For each segment, we calculate t_r as a function of HX height, h, width, w, and length l, laser scan speed, v, hatch spacing, H, layer thickness, L, and end of raster pause time, t_{rp}, as seen in Equation 7. The supplemental materials contain a detailed description of the build cycle time calculation. We use v 700 mm/s, H 110 microns, and L 40 microns. We assume t_{rp} 3 milliseconds per discussion with CMU NextManufacturing experts.

$$t_r = \frac{h}{L}\left[\frac{w}{H}\left(\frac{l}{v} + t_{rp}\right) + \frac{2(w+H)}{v} + 3t_{rp}\right] \tag{7}$$

We calculate powder spread time as a function of h, L, build plate length (250mm [26]), time to raise platform, t_{plat}, recoater spread speed v_{rs}, and recoater return speed v_{rr}. We use t_{plat} 2s, v_{rs} 150 mm/s and v_{rr} 500 mm/s.

$$t_{ps} = \frac{h}{L}\left(\frac{250}{v_{rs}} + \frac{250}{v_{rr}} + t_{plat}\right) \tag{8}$$

3.1.5. Labor Cost

For each process step, we calculate annual labor cost as a function of number of laborers, n_{lab}, annual salary, p_{lab}, and labor burden rate, r_{lab} (Equation 9).

$$c_{lab} = \frac{n_{lab}p_{lab}(1 + r_{lab})}{APV} \tag{9}$$

We use p_{lab} of \$36,000-88,000 based on salary ranges for an engineering technician [38]. For r_{lab}, we use the US average of 30% [39]. We calculate n_{lab} as a function of t_{mch}, labor fraction, f_{lab}, and annual manufacturing labor hours per full time laborer, t_{lab} (Equation 10). We estimate f_{lab} to be 3-13% for LPBF, 5% for heat treating, 26% for removing supports/base plate, and 50% for AFM. These numbers are calculated by estimating the ratio of the process that requires labor to the total duration of the process (see the supplemental materials for setup/teardown, heatup/cooldown, and cycle times and labor fractions). We assume t_{lab} of 1632 hrs.

$$n_{lab} = \frac{f_{lab}t_{mch}}{t_{lab}} \tag{10}$$

3.1.6. Facility Cost

For each process step, we calculate annual facility cost as a function of n_{mch}, floor space, A_{mch}, clearance space, A_{clr}, facility rental price p_{fac}, facility build out price p_{build}, and CRF (Equation 11). We use A_{mch} 16m^2 for LPBF [26], 5.4m^2 for heat treating [16], 16m^2 for removing supports/base plate [16], and 8m^2 for AFM [40]. We assume a clearance space of 200% A_{mch}. For p_{fac}, we use the US average industrial facility rent price of \$749/m^2 [41]. For p_{build}, we use \$4,300-5,400/m^2/month based on consultation with CMU NextManufacturing experts. We assume 20 yr amortization periods to calculate CRF for the facility build out.

$$c_{fac} = \frac{n_{mch}(A_{mch} + A_{clr})(p_{fac} + p_{build} * CRF)}{APV} \tag{11}$$

3.1.7. Consumables Cost

For each process step, we calculate the consumable materials used during the process as a function of consumable price, p_c, rate of consumption, r_c (either per hour of cycle time or per part), EPV, and t_{cyc} (for per hour-based r_c) (Equation 12). For LPBF, we model build plates (p_c \$700/plate [34], r_c 1 plate/10 HX) and filters(p_c \$600/filter set [34], r_c 1 filter set/3600 hrs). For removing supports/baseplate, we model blades (p_c \$190/blade [42], r_c 1 blade/1440 hrs) and cutting fluid (p_c \$8.40/L [43], r_c 60 L/hr[44]). Heat treating does not require consumables. For AFM, we model abrasive medium (p_c \$3500/machine fill, r_c 1 machine fill/machine/21,600 hrs (from vendor estimate)). All r_c values are based on estimates from equipment vendors and CMU NextManufacturing.

$$c_{cons} = \frac{\frac{p_c EPV t_{cyc}}{r_c}}{APV} \tag{12}$$

3.1.8. Utility Cost

We assume that the cost for all utilities except electricity are negligible. For each process step, we calculate annual utility cost as a function of t_{mch}, machine electricity use, r_{el}, and electricity price p_{el}. We use r_{el} of 16.7kW for LPBF [26], 6.2kW for heat treating [16], 7.8kW for removing supports/base plate [16], and 7.5kW for AFM [40]. For p_{el}, we use the US industrial electricity prices of \$0.067-0.248/kWh[45].

3.1.9. Overhead Cost

Overhead accounts for costs such as management, quality assurance, human resources, environmental health & safety, cleaning, accounting, administrative services, legal services, office space, inventory storage, building utilities (lights, heat, etc.), shipping/packing, office supplies, and IT equipment. We estimate total overhead cost based on typical small business costs for these goods and services. The supplemental materials contain a detailed description of the overhead calculation. At APV 1,500, overhead costs are equal to approximately 17% of total non-overhead costs. We distribute overhead cost across process steps by allocating a fraction of overhead cost to each step equal to the fraction of total non-overhead cost associated with that step.

4. Results

At an annual production volume (APV) of 1,500 units (required for a 20 MW CSP plant), our initial HX design costs approximately $780/kW-th ($660-780/kW-th). We broke down the HX cost by process step and cost category to identify opportunities to reduce HX cost.

The breakdown of HX cost per kW-th by manufacturing process step shows that the HX LPBF step is the most significant contributor to HX cost (Figure 2). The breakdown of cost by category shows that equipment is the most significant contributor to LPBF cost (Figure 2). Since LPBF equipment cost is dependent on print time (build cycle + heat-up/cooldown + set-up/teardown times), we also evaluated cost for various print times. This breakdown shows that cost in most LPBF cost categories decreases as build time decreases (Figure 2). We therefore focused our initial efforts to identify cost reduction opportunities on decreasing print time without changing HX performance.

Reducing the amount of material used in the HX will reduce the print time (and material cost). We evaluated reducing header volumes as the header geometry is not expected to substantially impact HX thermal performance. Reducing header volumes by 25% reduces cost to $600-720/kW-th. Reducing header volumes by 50% reduces cost to $540-640/kW-th. Based on this finding, we developed two alternative header designs, reducing header volume by 25 and 50% (Figure 3). Modeling of flow in the pin array showed that reducing the header volume does not substantially impact flow distribution uniformity within the pin array.

Varying LPBF processing parameters to increase build rate allows us to reduce build time, but also impacts porosity defect generation. Porosity measurements for various parameter sets (print speed, laser power, hatch spacing) from test builds in Haynes 282 show that two parameter sets minimize porosity (P 200W, v 760 mm/s, and P 250W, v 960 mm/s) (Figure 5). Increasing v to 960 mm/s lowers the HX cost by approximately \$100/kW-th. If parts with higher porosities maintain adequate mechanical properties, further increasing speed could reduce cost further. However, future work is needed to better understand the relationship between porosity and H282 material properties, such as creep performance.

Through the combination of the header re-design and increased laser scan speed of 960 mm/s, we can reduce the HX cost to \$530-610/kW-th. With these changes, the AM process step is still the largest contributor to total cost.

To identify further avenues for cost reduction, we evaluated scenarios that can likely be achieved using currently commercially available technologies. Analyzed scenarios include: improved powder removal methods to reduce fraction of trapped powder, leveraging production LPBF machine monitoring software to reduce required human monitoring, and using multi-laser machines to reduce print time. [46, 47, 48] Table 1 describes these scenarios. Implementation of LPBF process modifications enabled by commercially available technologies could reduce HX cost further to approximately \$400-450/kW-th (Figure 4).

A number of innovations in LPBF machines are currently under development to improve print time and support production-scale LPBF. We evaluate scenarios that may be enabled by these future innovations. These scenarios include: increasing laser scan speed through higher power lasers, spot size control, or beam shaping, reducing setup/teardown time with automated setup and compartmentalized machines, reducing heatup/cooldown time with dedicated cooling compartments, and improving part acceptance through lean/six-sigma process improvement.[49, 50, 51, 52] Table 1 describes these scenarios. If these scenarios are realized, they could lower HX cost further to \$240-290/kW-th (Figure 4).

Table 1: Scenarios modifying AM manufacturing process parameters. Short-term scenarios are likely possible with current commercially available technologies. Long-term scenarios may be possible in the future with innovations currently in development.

Scenario	**Description**	**Variable Changed**	**Baseline Value**	**Scenario Value**
Short-term Cost Reduction (enabled by current commercial technologies)				
Recover trapped powder	Recover and recycle unmelted powder trapped in plates*	trapped powder recycle fraction	0%	90%
1% Build cycle monitoring	Reduce portion of the build cycle that must be monitored by a laborer**	cycle labor fraction	10%	1%
EOS M400-4	Switch to EOS M400-4 AM machine with 4 lasers and larger build area	raster time	t_r	$\frac{1}{4}t_r$
		build plate length	250 mm	400 mm
		machine price	\$595k	\$1.66m
Long-term Cost Reduction (enabled by techniques and technologies under development)				
1400 mm/s speed	Increase laser scan speed (from 960 mm/s speed in short-term reduction)	laser scan speed	960 mm/s	1400 mm/s
90% Setup/teardown reduction	Reduce time required to load and unload AM machine	setup/teardown time	4.5hr	0.5 hrs
90% Heatup/cooldown reduction	Reduce time required for LPBF machine pre-heating and cooldown	heatup/cooldown time	5hr	0.5hr
2800 mm/s speed	Increase laser scan speed (marginal cost reduction for increasing from 1400 to 2800 mm/s)	laser scan speed	1400 mm/s	2800 mm/s
99% Part acceptance	Reduce fraction of defective parts produced in 3D printing HX	part acceptance rate	90%	99%

*Removal of trapped powder has been demonstrated in laboratory without additional equipment.
**Software license cost is negligible relative to overall part cost.

After evaluating options to reduce HX cost without changing HX performance, we evaluated an alternative HX design as an option to reduce cost. The alternative design introduces a pin array to the MS-side to increase HX performance, and moves the headers to the side of the HX allowing for stacks of multiple units to be printed (Figure 6). This design reduces cost to $220-260/kW-th for printing at 700 mm/s and $200-240/kW-th for printing at 960 mm/s (Figure 7). We evaluated the impact of technological innovation and manufacturing process optimization scenarios on the alternative design (Figure 8). If these scenarios are realized, they could lower HX cost for the alternative design to $130-170/kW-th.

5. Conclusions

We demonstrate the potential for AM, specifically LPBF, to meet the performance challenges presented by the primary HX for CSP systems with MS thermal energy storage in a cost effective manner. We initially find that if the HX is produced with a conservative, lab-based process it would cost $780/kW-th ($650-790/kW-th). We demonstrate that by integrating cost modeling into the design and LPBF parameter selection process, it is possible to significantly reduce costs for the HX:

- Reducing the volume of the HX headers by 50% and increasing laser scan speed from 700 mm/s to 960 mm/s, reduces the cost to $530-610/kW-th.
- Incorporating additional LPBF process modifications possible with commercially available industrial scale LPBF technologies,reduces cost to $400-450/kW-th.
- LPBF machine innovations recently brought to market or currently under development could cut HX cost to $240-290/kW-th.
- Redesigning the HX based on cost model insights reduces HX cost $200-230/kW-th (at 960 mm/s without any additional LPBF process or machine modifications).
- Incorporating LBPF machine innovations and manufacturing process optimizations could reduce cost for the redesigned HX to $130-170/kW-th. This cost range is consistent with a $150/kW-th target for the CSP

primary HX cost required to achieve a cost competitive CSP system as identified by identified by Mehos et. al [53] and Vijaykumar et. al. [54].

While this manuscript focuses on demonstrating the economic viability of fabricating an MS-to-SCO_2 HX for CSP via LPBF, our integrated approach to design, manufacturing process parameter selection, and cost could be applied to develop cost-effective solutions to other clean energy manufacturing challenges using AM.

6. Acknowledgements

Funding for these projects was provided by the Solar Energy Technologies Office under contract DE-EE0008536 and the Advanced Research Projects Agency - Energy under contract DE-AR0001127.

We additionally thank Todd Baer, Sandra DeVincent Wolf, Michael Kelly, Jeffrey Harris, Stephen Mrdjenovich, and Penny Toniolo for their consultation on inputs used in our cost model.

References

[1] C. DOE, Quadrennial technology review 2015—chapter 6: Innovating clean energy technologies in advanced manufacturing—composite materials (2015).

[2] M. Mehos, C. Turchi, J. Jorgenson, P. Denholm, C. Ho, K. Armijo, On the Path to SunShot: Advancing Concentrating Solar Power Technology, Performance, and Dispatchability, SunShot (May) (2016) 1–66.

[3] DOE, Concentrating solar power, `https://www.energy.gov/sco2-power-cycles-renewable-energy-applications/concentrating-solar-power`, (Accessed on 12/20/2020).

[4] HEXCES, Hexces - technology, `http://www.hexces.com/technology`, (Accessed on 12/19/2020).

[5] J. Nestell, T. L. Sham, Asme code considerations for the compact heat exchanger, Oak Ridge National Laboratory, ORNL/TM-2015/401 (2015).

[6] M. Kapoor, K. Rozman, O. Dogan, J. Hawk, R. Saranam, P. McNeff, B. Paul, Diffusion bonding of h230 ni-superalloy for application in microchannel heat exchanger, Tech. rep., NETL (2016).

[7] I. Gibson, D. W. Rosen, B. Stucker, et al., Additive manufacturing technologies, Vol. 17, Springer, 2014.

[8] E. Rasouli, C. Davis, S. Subedi, C. Montgomery, C. Mande, W. C. E. Center, M. Stevens, V. Narayanan, A. Rollett, Design and performance characterization of an additively manufactured primary heat exchanger for sco2 waste heat recovery cycles, in: Proceedings of the 6th International Symposium on Supercritical CO2 Power Cycles, Pittsburgh, PA, USA, 2018, pp. 27–29.

[9] D. Singh, W. Yu, D. M. France, T. P. Allred, I.-H. Liu, W. Du, B. Barua, M. C. Messner, One piece ceramic heat exchanger for concentrating solar power electric plants, Renewable Energy 160 (2020) 1308–1315.

[10] D. Saltzman, M. Bichnevicius, S. Lynch, T. W. Simpson, E. W. Reutzel, C. Dickman, R. Martukanitz, Design and evaluation of an additively manufactured aircraft heat exchanger, Applied Thermal Engineering 138 (2018) 254–263.

[11] M. A. Arie, A. H. Shooshtari, M. M. Ohadi, Experimental characterization of an additively manufactured heat exchanger for dry cooling of power plants, Applied Thermal Engineering 129 (2018) 187–198.

[12] R. Tiwari, R. S. Andhare, A. Shooshtari, M. Ohadi, Development of an additive manufacturing-enabled compact manifold microchannel heat exchanger, Applied Thermal Engineering 147 (2019) 781–788.

[13] F. Field, R. Kirchain, R. Roth, Process cost modeling: Strategic engineering and economic evaluation of materials technologies, Jom 59 (10) (2007) 21.

[14] R. Kirchain, F. Field, Process-based cost modeling: understanding the economics of technical decisions, Encyclopedia of Materials Science and Engineering 2 (2001) 1718–1727.

[15] E. R. Fuchs, F. R. Field, R. Roth, R. E. Kirchain, Strategic materials selection in the automobile body: Economic opportunities for polymer composite design, Composites science and technology 68 (9) (2008) 1989–2002.

[16] R. E. Laureijs, J. B. Roca, S. P. Narra, C. Montgomery, J. L. Beuth, E. R. Fuchs, Metal additive manufacturing: cost competitive beyond low volumes, Journal of Manufacturing Science and Engineering 139 (8) (2017).

[17] H. Benson-Woodward, M. Koslowske, R. Kirchain, I. Bar-On, A performance based, multi-process cost model for solid oxide fuel cells, MRS Proceedings 756 (2002) FF4.10. doi:10.1557/PROC-756-FF4.10.

[18] A. Sakti, J. J. Michalek, E. R. Fuchs, J. F. Whitacre, A techno-economic analysis and optimization of li-ion batteries for light-duty passenger vehicle electrification, Journal of Power Sources 273 (2015) 966–980.

[19] Z. Nie, S. Jung, L. B. Kara, K. S. Whitefoot, Optimization of part consolidation for minimum production costs and time using additive manufacturing, Journal of Mechanical Design 142 (7) (2020).

[20] E. Ulu, R. Huang, L. B. Kara, K. S. Whitefoot, Concurrent structure and process optimization for minimum cost metal additive manufacturing, Journal of Mechanical Design 141 (6) (2019).

[21] Q. Gao, J. Lizarazo-Adarme, B. K. Paul, K. R. Haapala, An economic and environmental assessment model for microchannel device manufacturing: part 1–methodology, Journal of cleaner production 120 (2016) 135–145.

[22] Q. Gao, J. Lizarazo-Adarme, B. K. Paul, K. R. Haapala, An economic and environmental assessment model for microchannel device manufacturing: part 2–application, Journal of Cleaner Production 120 (2016) 146–156.

[23] B. Paul, C. Song, K. Lee, B. M. Fronk, D. Sahoo, M. Shipley, Conceptual design of a manufacturing process for an automotive microchannel heat exchanger (2018).

[24] Haynes Internations, Haynes 282 Alloy (2020).

[25] I.-N. Tano, E. Rasouli, T. Ziev, Z. Wu, N. Lamprinakos, J. Seo, L. S. Balhorn, P. Vaishnav, A. Rollett, V. Narayanan, An additively-manufactured molten salt-to-supercritical carbon di-oxide primary heat exchanger for solar thermal power generation–design and techno-economic performance, Solar Energy 234 (2022) 152–169.

[26] EOS GmbH, Technical data - eos m 290, https://www.eos.info/en/additive-manufacturing/3d-printing-metal/eos-metal-systems/eos-m-290, (Accessed on 05/05/2020) (1 2019).

[27] T. M. Mower, M. J. Long, Mechanical behavior of additive manufactured, powder-bed laser-fused materials, Materials Science and Engineering: A 651 (2016) 198–213.

[28] A. B. Spierings, T. L. Starr, K. Wegener, Fatigue performance of additive manufactured metallic parts, Rapid prototyping journal (2013).

[29] H. Gong, K. Rafi, H. Gu, T. Starr, B. Stucker, Analysis of defect generation in ti–6al–4v parts made using powder bed fusion additive manufacturing processes, Additive Manufacturing 1 (2014) 87–98.

[30] R. W. Cunningham, Defect formation mechanisms in powder-bed metal additive manufacturing, Ph.D. thesis, Carnegie Mellon University (2018).

[31] M. Tang, P. C. Pistorius, J. L. Beuth, Prediction of lack-of-fusion porosity for powder bed fusion, Additive Manufacturing 14 (2017) 39–48.

[32] J. V. Gordon, S. P. Narra, R. W. Cunningham, H. Liu, H. Chen, R. M. Suter, J. L. Beuth, A. D. Rollett, Defect structure process maps for laser powder bed fusion additive manufacturing, Additive Manufacturing 36 (2020) 101552.

[33] NextManufacturing Carnegie Mellon University, Details and cost, https://engineering.cmu.edu/next/facilities/details-cost.html, (Accessed on 05/07/2020).

[34] Phillips Corporation Federal Division, Gs-03f-080ca phillips federal price list schedule 2020, https://www.gsaadvantage.gov/ref_text/GS03F080CA/

0VGL91.3R6Y7S_GS-03F-080CA_GS03F080CAPHILLIPSFEDERAL 07012020.PDF, (Accessed on 12/19/2020) (7 2020).

[35] DGI Supply, Doall dc-400cnc, https://www.dgisupply.com/product/CMIDC400CNC/;pgidj̄kXWMVB7ulZSRphasW29_Dxt0000Mbr-8vXP;sidP̄u3DRFWI27XIRA7k -4gkR0UkXEYNUshmvgJeqtVn, (Accessed on 12/22/2020).

[36] K. S. Fujita, Commercial discount rate estimation for efficiency standards analysis (2016).

[37] D. M. Dietrich, M. Kenworthy, E. A. Cudney, Additive Manufacturing Change Management: Best Practices, CRC Press, 2019.

[38] US Bureau of Labor Statistics, Engineering technicians, except drafters, all other, https://www.bls.gov/oes/2017/may/oes173029.htm, (Accessed on 11/11/2020) (05 2017).

[39] US Bureau of Labor Statistics, Employer costs for employee compensation for the regions – december 2019, https://www.bls.gov/regions/southwest/news-release/employercostsforemployee compensation_regions.htm, (Accessed on 05/07/2020) (12 2019).

[40] ExtrudeHone, Product data sheet vector, https://extrudehone.com/wp-content/uploads/2016/04/15001_EH_VECTOR_v06_Final.pdf, (Accessed on 05/07/2020).

[41] Statista, Industrial rents per square foot by type u.s. 2018, https://www.statista.com/statistics/626555/average-rent-per-square-foot-paid-for-industrial-space-usa-by-type/, (Accessed on 05/05/2020) (11 2019).

[42] Global Industrial, Band saw blades, https://www.globalindustrial.com/c/metalworking-tools/metalworking-saw-blades/bandsaw-blades, (Accessed on 12/19/2020).

[43] Global Industrial, Metal working fluids, https://www.globalindustrial.com/c/metalworking-tools/metal-fluids/metalworking-fluids-2, (Accessed on 12/19/2020).

[44] B. Denkena, P. Helmecke, L. Hülsemeyer, Energy efficient machining with optimized coolant lubrication flow rates, Procedia CIRP 24 (2014) 25–31.

[45] US Energy Information Administration, Electric Power Monthly with data for February 2020, Tech. rep.

[46] Solukon, Solukon - metall, https://www.solukon.de/en/metall/, (Accessed on 12/23/2020).

[47] EOS GmBH, 3d printing software. industrial solutions for am production, https://www.eos.info/en/additive-manufacturing/software-3d-printing, (Accessed on 12/23/2020).

[48] EOS GmbH, EOS M400-4, https://www.eos.info/en/additive-manufacturing/3d-printing-metal/eos-metal-systems/eos-m-400-4, (Accessed on 12/22/2020).

[49] SLM, SLM NXG XII 600 Detail Page, https://www.slm-pushing-the-limits.com/specs, (Accessed on 12/23/2020).

[50] TRUMPF, TruPrint Series 5000, https://www.trumpf.com/en_US/products/machines-systems/additive-production-systems/truprint-5000/, (Accessed on 12/23/2020).

[51] R. Shi, S. A. Khairallah, T. T. Roehling, T. W. Heo, J. T. McKeown, M. J. Matthews, Microstructural control in metal laser powder bed fusion additive manufacturing using laser beam shaping strategy, Acta Materialia 184 (2020) 284–305.

[52] H. Yang, P. Rao, T. Simpson, Y. Lu, P. Witherell, A. R. Nassar, E. Reutzel, S. Kumara, Six-sigma quality management of additive manufacturing, Proceedings of the IEEE (2020).

[53] M. Mehos, C. Turchi, J. Vidal, M. Wagner, Z. Ma, C. Ho, W. Kolb, C. Andraka, A. Kruizenga, Concentrating solar power gen3 demonstration roadmap, Tech. rep., National Renewable Energy Lab.(NREL), Golden, CO (United States) (2017).

[54] R. Vijaykumar, M. L. Bauer, M. Lausten, A. M. Shultz, Optimizing the supercritical co2 brayton cycle for concentrating solar power application, in: Proceedings of the 6th Int Symp—Supercrit CO2 Power Cycles, Pittsburgh, PA, USA, 2018, pp. 27–29.

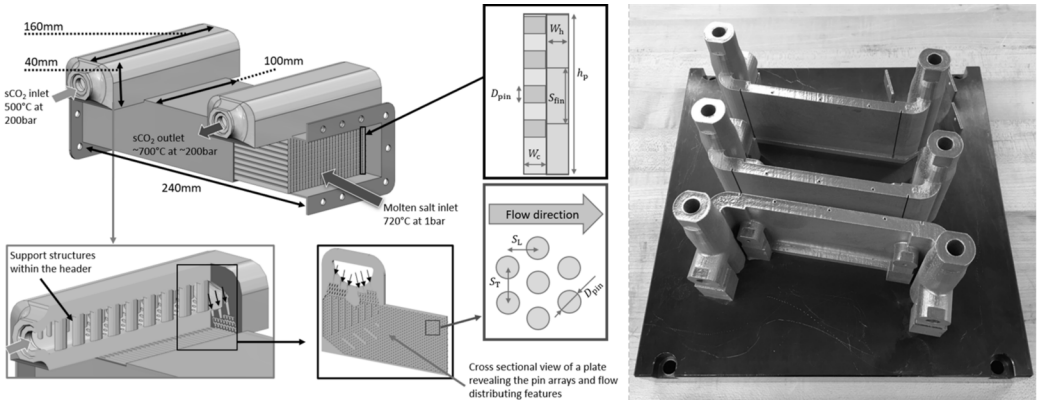

Figure 1: Left: HX design with sections showing of header internals and sCO_2 side micropin features. Right: The as-built single channel H282 HX units on an EOS M290 build plate.

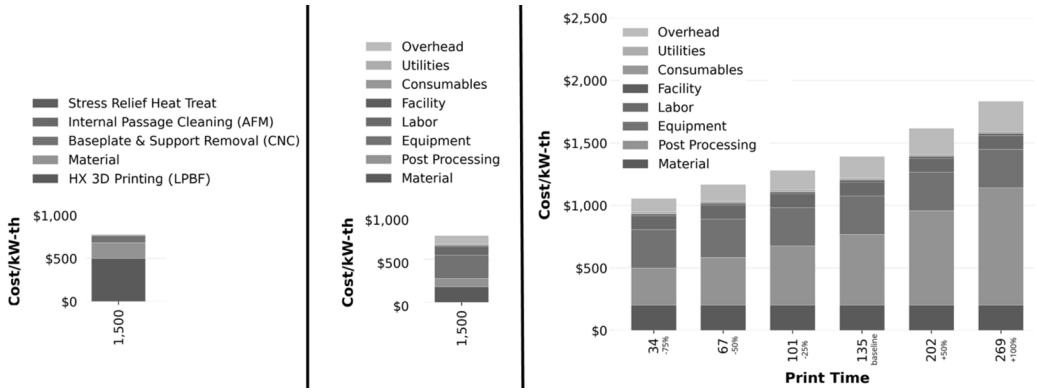

Figure 2: Left: Breakdown of initial HX design cost by process step for various APV. LPBF is the most significant contributor to HX cost. Center: Breakdown of initial HX design cost with HX LPBF cost categories for various APV. The most significant driver of LPBF cost is equipment cost. Right: Breakdown of initial HX design cost for various print times (baseline print time is 135 hrs). Contributors to LPBF cost can be reduced by reducing print time.

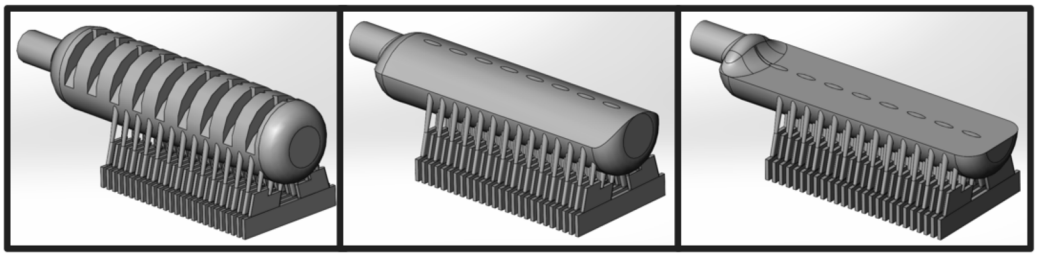

Figure 3: Internal design of header for: initial HX design (left), 25% volume reduction (center), and 50% volume reduction (right).

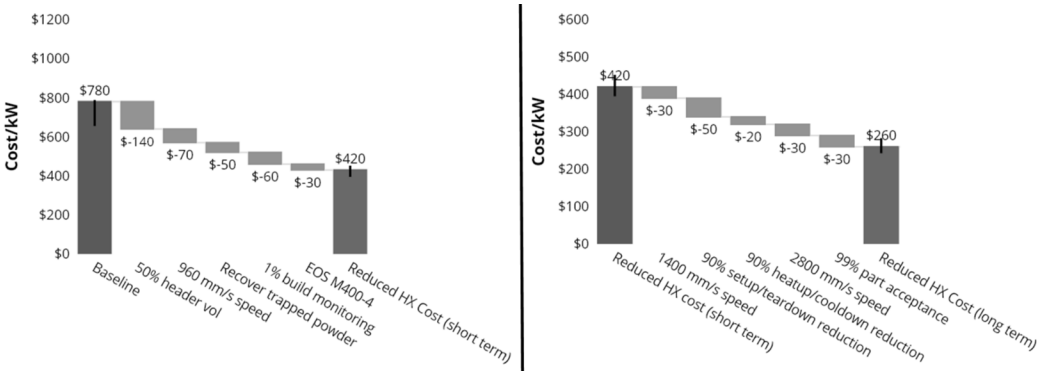

Figure 4: Left: Cost reductions achieved through various measures that are likely feasible with current commercially available technology. Measures are arranged by likelihood to be immediately implementable with those that are most likely on the left. Right: Cost reductions achieved through various measures that are may be feasible with medium-term technological innovation. Measures are arranged by likelihood to implementable in the longer term with those that are most likely on the left. Table 1 contains a description of each scenario.

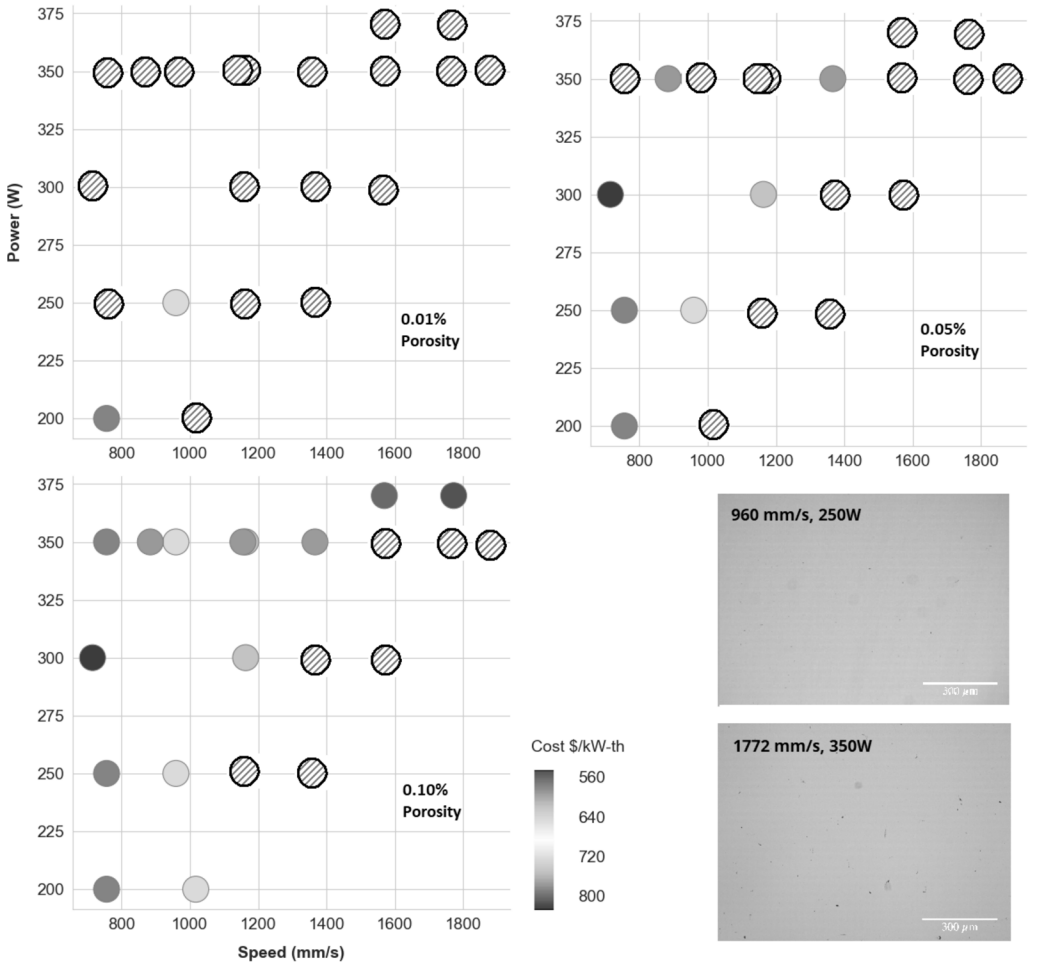

Figure 5: Each spot in these figures represents the cost/kW associated with producing HX in H282 with the given P and v parameter set. In each panel, test samples that exceeded the porosity threshold for that panel are blacked out. L for all parameter sets is 40 microns. H for all parameter sets is 110 microns except (884,350 - H 170), (1155,350 - H 130), and (1878,350 - H 80). Costs shown assume 1,500 unit APV. The optical micrographs show the polished cross-sections of the as-built H282 specimens 3D printed vua LPBF at (960,250 - H 110) and (1772,350 - H 110) which highlight the subtle change of porosity content at different build rates.

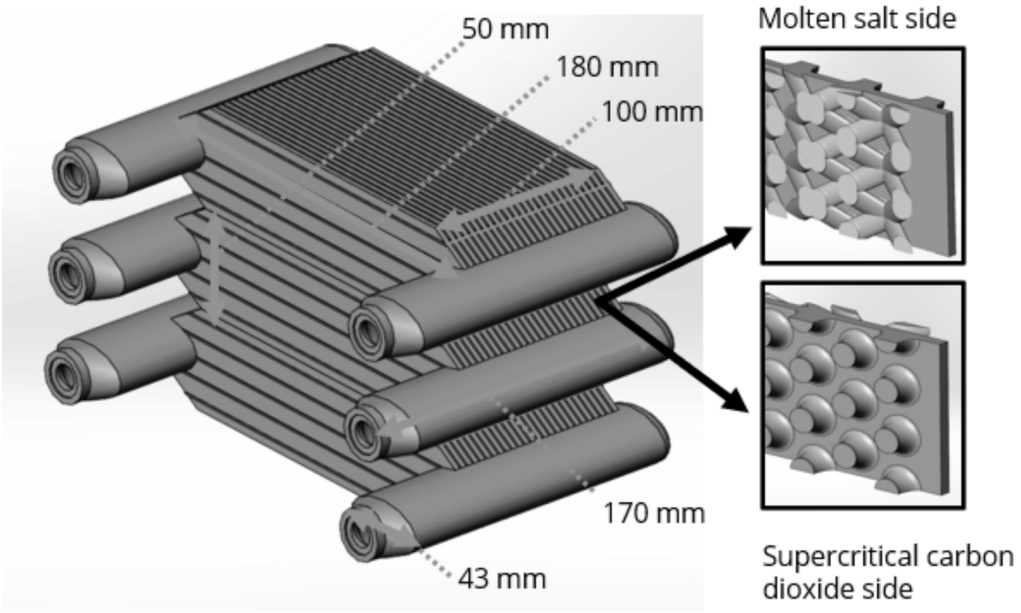

Figure 6: Alternative HX design showing a stack of three units with sections showing the MS and sCO_2 side micropin features.

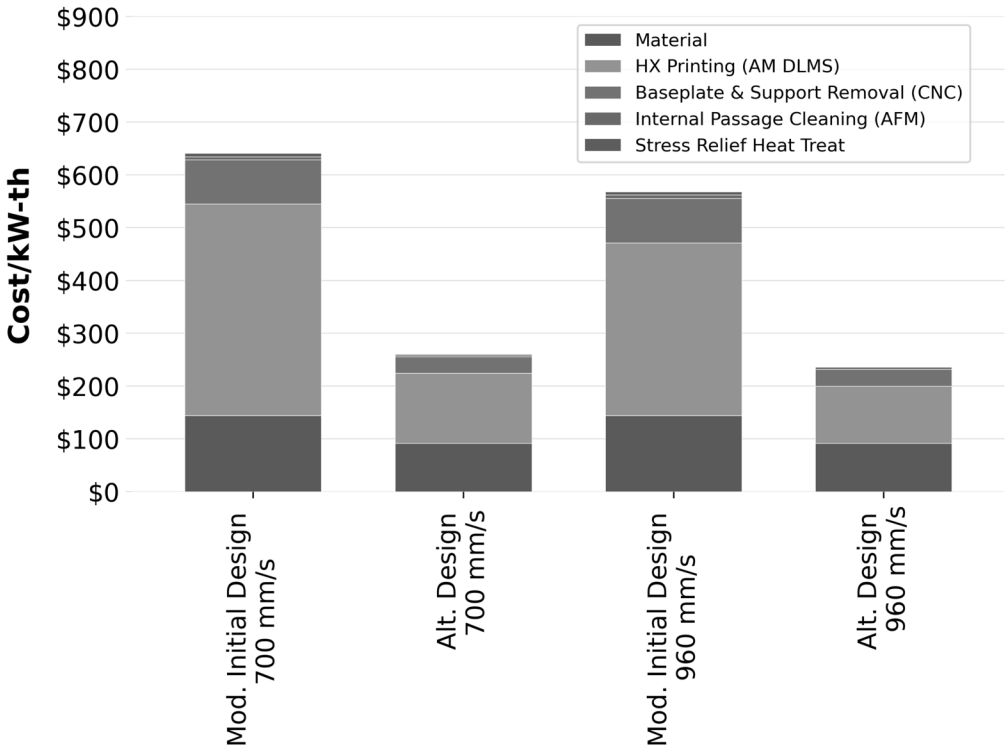

Figure 7: Breakdown of cost by process step for the modified initial and alternative HX designs at 700 and 900 mm/s print speeds.

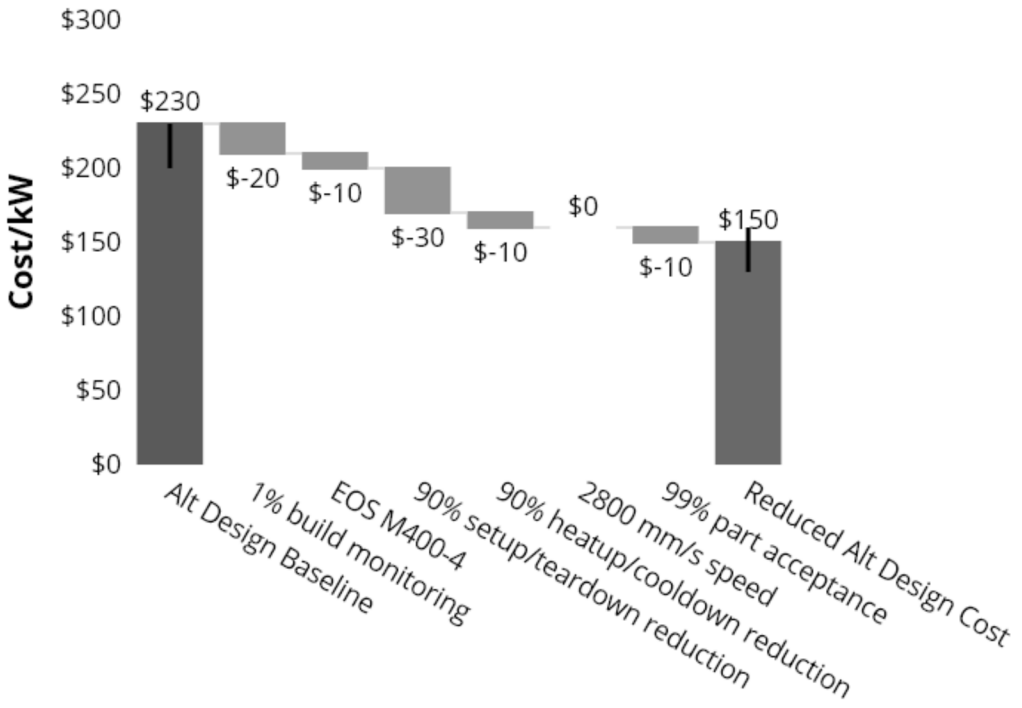

Figure 8: Cost reductions achieved through various technological innovations and manufacturing process optimizations. Table 1 contains a description of each scenario.

Economics of Using Additive Manufacturing to Fabricate a Molten Salt-to-Supercritial Carbon Dioxide Heat Exchanger for Concentrating Solar Power

Tracey Ziev, Erfan Rasouli, Ines-Noelly Tano, Ziheng Wu, Srujana Rao Yarasi, Nicholas Lamprinakos, Junwon Seo, Vinod Narayanan, Anthony D. Rollett, Parth Vaishnav

1 PBCM Inputs and Assumptions

1.1 Assumptions

1.1.1 General

- Operating hours: 24/7 operation for 49 weeks/yr to account for maintenance activities, holidays, and other plant closures.
- Discount rate: US small industrial business average rate.
- Quality Control: all defective parts identified after final step of entire manufacturing process.

1.1.2 Materials

- H282 density: Assume same as H282 non-powdered material.
- Scrap: no cost/revenue from disposal/recycle of scrap material.
- Scrap: no scrap generated outside HX 3D printing.
- 3D printing material use: For baseline, no powder can be recycled from hollow areas from within plates (between pins).

1.1.3 Equipment

- Equipment dedication: assume all equipment is only used for modeled part.
- Installation cost: one time 10% of capital cost if no installation cost input available.
- Equipment operating life: 20 yrs if no operating life input life available.
- Maintenance cost: 5% of capital cost per year if no maintenance cost input available.
- Working floor space: 2x actual equipment floor size.
- Machine downtime: no downtime outside plant-wide maintenance shutdowns.
- EOS M400-4: machine labor fractions, set up/tear down times, and heat up/cool down times are the the same as EOS M290.

1.1.4 HX Print Time

- Layer melt time: single raster direction (in direction of powder spread)
- Support structures: negligible support structures are required and are therefore not modeled.

1.1.5 Labor

- Salary: can be approximated by US national 75th percentile manufacturing technician salary. (75th% rather than average chosen to account for higher skill level required for AM.)
- Labor burden: can be approximated as fraction of salary, with fraction approximated by US average burden fraction.
- Labor hours: workers use 85% of time in production capacity to account for breaks, shift turn over, training, admin activities, etc.
- Labor dedication: assume workers are can work on any process step, but only for modeled part (unused labor hours accounted as overhead cost).

1.1.6 Facility

- Facility rent: can be approximated by US national average.

1.1.7 Consumables

- AM machine recoater blades: included in maintenance contract [1].
- Heat Treating: no specialized fixtures required.
- CNC: no recycling of cutting fluid.
- CNC: saw blade life 2 months.
- AFM: fixture costs for connecting HX are negligible (per vendor discussion, it may be possible to connect HX without specialized tooling due to connectors present in HX design).
- AFM: after initial machine fill, 20% abrasive medium is replaced every 6 months (per vendor estimate).
- EOS M400-4: Consumables has same usage rate as EOS M290.

1.1.8 Utilities

- Modeled Utilities: non-electricity utilities contribute negligibly to cost and are therefore not modeled.
- Electricity price: can be approximated by US national average.

1.1.9 Overhead

- Inputs for overhead cost calculations can be approximated by US small business and small manufacturer average costs.
- Add 10% total overhead cost to account for unmodeled costs.

- See overhead section of inputs for detailed list of assumed overhead inputs.
- See Appendix 3 for assumptions regarding relationship of overhead inputs, manufacturing process, and cost.

1.2 Inputs

Name	Value	Source
General		
Annual operating hours	8064	assumed
Discount rate	8.5%	[2]
Materials		
H282		
Density	8,270 kg/m^3	[3]
Price	\$125-145/kg	vendor quote
Equipment		
AM Machine - EOS M290		
Machine price	\$535,000-700,000	[1]
Installation cost	\$47,000	[1]
Machine life	7-10 yrs	[4]
Maintenance cost	\$58,000/yr	[1]
Build chamber height	325mm	[5]
Build chamber length	250mm	[5]
Build chamber width	250mm	[5]
Set up/teardown time	4.5 hr	CMU NextManufacturing
Set up/teardown labor fraction	1.0	CMU NextManufacturing
Cycle labor fraction	0-0.10	CMU NextManufacturing
Floor space	3.25 m^2	[5]
Scrap rate	5-15% part material	[6]
Part acceptance rate	80-95%	AM expert input
Electricity consumption	16.7 kW	[5]
Heat up/cool down time	5 hr	CMU NextManufacturing
Heat up/cool down labor fraction	0.1	CMU NextManufacturing
AM Machine - EOS M400-4		
Machine price	\$1,662,000	[1]

Name	Value	Source
Installation cost	$57,300	[1]
Machine life	7-10 yrs	[4]
Maintenance cost	$90,900/$yr$	[1]
Build chamber height	400mm	[7]
Build chamber length	400mm	[7]
Build chamber width	400mm	[7]
Set up/teardown time	4.5 hr	assumed
Set up/teardown labor fraction	1.0	assumed
Cycle labor fraction	0-0.10	assumed
Floor space	6.8 m^2	[7]
Scrap rate	5-15% part material	[6]
Part acceptance rate	80-95%	AM expert input
Electricity consumption	45 kW	[7]
Heat up/cool down time	5 hr	assumed
Heat up/cool down labor fraction	0.1	assumed
Heat Treatment Furnace		
Machine price	$50,000	[8]
Installation cost	$5,000	assumed
Machine life	Avg: 20 yrs	assumed
Maintenance cost	$2,500/$yr$	assumed
Set up/teardown time	0.1 hr	CMU NextManufacturing
Set up/teardown labor fraction	1.0	CMU NextManufacturing
Cycle time	4 hrs	set by collaborators
Cycle labor fraction	0.0	CMU NextManufacturing
Floor space	5.4 m^2	[8]
Scrap rate	None	assumed
Part acceptance rate	100%	CMU NextManufacturing
Electricity consumption	6.2 kW	[8]
Heat up/cool down time	8 hr	CMU NextManufacturing
Heat up/cool down labor fraction	0.0	CMU NextManufacturing
CNC Band Saw		
Machine price	$64,890	[9]
Installation cost	$6,500	assumed

Name	Value	Source
Machine life	Avg: 20 yrs	assumed
Maintenance cost	\$3,250/yr	assumed
Set up/teardown time	0.25 hr	[10]
Set up/teardown labor fraction	1.0	assumed
Cycle labor fraction	0.0	assumed
Cycle time	1hr	[10]
Floor space	7.8 m^2	[9]
Scrap rate	None	assumed
Part acceptance rate	98%	[10]
Electricity consumption	6.6 kW	[9]
Vector AFM		
Machine price	\$170,000	vendor estimate
Installation cost	\$17,000	assumed
Machine life	Avg: 20 yrs	assumed
Maintenance cost	\$8,500/yr	assumed
Set up/teardown time	0.5 hr	vendor estimate
Set up/teardown labor fraction	1.0	vendor estimate
Cycle labor fraction	0.0	vendor estimate
Cycle time	0.0	vendor estimate
Floor space	7.8 m^2	[11]
Scrap rate	None	assumed
Part acceptance rate	99%	vendor estimate
Electricity consumption	7.5 kW	[11]
Labor		
Annual manufacturing hours	1,632/laborer	assumed
Labor burden cost rate	30%	[12]
Manufacturing technician salary	\$36,000-88,000	[13]
Facility		
Manufacturing facility rent	Avg: \$749/m^2/yr	[14]
Consumables		
EOS M290		
Baseplate price	\$700/piece	[1]
Baseplate life	10 uses	CMU NextManufacturing
Filter price	\$600/piece	[1]

Name	Value	Source
Filter life	3600 hrs	CMU NextManufacturing
EOS M400-4		
Baseplate price	$715/piece	[1]
Baseplate life	10 uses	assumed
Filter price	$615/piece	[1]
Filter life	3600 hrs	assumed
CNC Band Saw		
Blade price	$193/piece	[15]
Blade life	1440 hrs	assumed
Cutting fluid price	$8.4/L	[16]
Cutting fluid usage	60 L/hr	[10], [17]
Vector AFM		
Abrasive medium price	$3,500/machine	vendor estimate
Abrasive medium life	60 months	vendor estimate
Utilities		
Electricity Cost	Avg: $0.067-0.248/$kWh$	[18]
Overhead		
Ratio supervisors to laborers	0.1	assumed
Supervisor salary	$110,000/yr	[19]
Fraction parts subject to QA inspection	0.2	assumed
Time for QA inspection	0.25hrs	assumed
QA salary	$40,000/yr	[20]
Regulatory compliance costs	$18,000/yr	[21]
Legal services price	$250/hr	[22]
Legal service use rate	0.025/HX	assumed 40hrs/1,500 HX order
Insurance price	$6,000/yr	[23]
HR services price	$300/employee/year	[24]
Cleaning services price	$1.64/$m^2$	[25]
Administrative employee to laborer ratio	0.1	assumed
Administrative salary	$39,000/yr	[26]
Accounting price	$1,500/yr	[27]

Name	Value	Source
Office space	15.9 m^2/employee	[28]
Office build out cost	\$24,400/office	[28]
Office build out life	10 yrs	assumed [29]
Packaging price	\$400/HX	[30]
Inventory storage	\$750/HX	assumed
IT and software costs	\$6,800/yr/employee	[31]
Office supplies cost	\$600/yr/employee	[32]

2 HX Print Time Calculation

As discussed in the Methods section of this paper, we divide the HX into constant cross-section segments and apply Equation 1 to calculate the raster time to each section. The sections we chose are header, header connector, plate, pin, and fin, the dimensions of which are listed in the table included at the end of this Appendix. The dimensions are listed so that for each section, h is the dimension in the build direction and w is the dimension in the powder spread direction. For each solid section (i.e. when all inner dimensions are 0 mm), we directly apply Equation 1 to the outer dimensions, For each hollow section, we subdivide the section into three parts: front/back, top/bottom, and sides. For each of these sections, we use placeholder dimensions, $h*$, $l*$, and $w*$. We apply Equation 7 from the paper to each subsection, then calculate the total section raster time per Equation 8 from the paper.

$$t_r = 2t_{f/b} + 2t_{t/b} + 2t_{side} \tag{1}$$

We then calculate the total t_r for the HX as:

$$t_r = n_{header}(t_{header} + t_{connector}) + n_{plate}tplate + n_{fin}t_{fin} + n_{pin}tpin \tag{2}$$

Dimension	Value	Dimension	Value
Pin Array		**Plates**	
# Plates	26	Outer width	2.8 mm
# Fins	234	Inner width	1.8 mm
# Pins	17,732	Outer height	50.5 mm
# Headers	2	Inner height	48.5 mm
$\dot{Q}$	12.7 kW	Outer length	240 mm
		Inner length	240 mm
		Plate spacing	1.0 mm

Dimension	Value	Dimension	Value
Headers		**Connectors on Headers**	
Outer width	160 mm	Outer width	37.5 mm
Inner width	150 mm	Inner width	37.5 mm
Outer height	60 mm	Outer height	25 mm
Inner height	40 mm	Inner height	15.75 mm
Outer length	60 mm	Outer length	30 mm
Inner length	40 mm	Inner length	15.75 mm
Fins		**Pins**	
Outer width	1.0 mm	Outer width	1.2 mm
Inner width	0.0 mm	Inner width	0.0 mm
Outer height	1.0 mm	Outer diameter	1.2 mm
Inner height	0.0 mm	Inner diameter	0.0 mm
Outer length	240 mm	Pin spacing	2.6 mm
Inner length	0.0 mm		
Fin spacing	4.0 mm		
Subsections			
Front/Back	$h* = h_{outer}$	$w* = \frac{w_{outer}-w_{inner}}{2}$	$l* = l_{outer}$
Top/Bottom	$h* = \frac{h_{outer}-h_{inner}}{2}$	$w* = w_{outer}$	$l* = l_{outer}$
Sides	$h* = h_{inner}$	$w* = w_{inner}$	$l* = \frac{}{2}$

3 Overhead Calculation

In our initial approach, we intended to estimate overhead cost as a fraction of labor expenses. However, after searching for an appropriate overhead multiplier, we found that estimates of typical overhead costs in manufacturing range from 20 to 300% [33], [34]. To narrow this band, we developed an approximate model to estimate overhead costs based on the inputs listed in Appendix 1. We acknowledge that this estimate is uncertain and very dependent on assumptions. However, this estimate is still valuable for helping judge the appropriate order of magnitude for the overhead costs associated manufacturing the HX. In future uncertainty quantification work, we will vary the size of the overhead estimate to account for this uncertainty.

To calculate the total overhead cost, we sum our estimates for the following costs:

- Unused labor hours (resulting from assumption that laborers dedicated for manufacturing HX)
- Management

- Quality assurance
- Regulatory compliance
- Legal services
- Insurance
- Human resources
- Administrative services
- Cleaning services
- Accounting services
- Office space
- Office supplies
- IT and software
- Inventory storage space
- Packaging
- General building utilities

We assume the following to be flat annual costs:

- Insurance
- Accounting services

We assume the following costs to be a per employee per year:

- HR services
- Office supplies
- IT and software

We assume the following costs to be per part:

- Legal services
- Packaging
- Inventory storage space

We assume the following costs to be per m^2 of facility space:

- Cleaning services

- Building utilities

We calculate management cost as:

$$c_{mgmt} = r_{mgmt} n_{lab} p_{mgmt} \tag{3}$$

where r_{mgmt} is the ratio of managers/supervisors to laborers, n_{lab} is the number of labors required for the manufacturing process, and p_{mgt} is the salary for managers.

We calculate quality assurance cost as:

$$c_{qa} = r_{qa} p_{qa} \frac{EPV t_{qa}}{t_{lab}} \tag{4}$$

where r_{qa} is the fraction of parts requiring QA inspection, p_{qa} is the salary of a QA/QC inspector, and t_{qa} is the time required to complete a QA inspection.

We calculate administrative services cost as:

$$c_{adm} = r_{adm} n_{lab} p_{adm} \tag{5}$$

where r_{adm} is the ratio of administrative employees to laborers and p_{adm} is the salary for managers.

we calculate the number of offices required as:

$$n_{off} = r_{off} * n_{emp} \tag{6}$$

where r_{off} is the amount of office space per employee and n_{emp} is the total number of employees. We then calculate office space costs as:

$$c_{off} = n_{off}(CRF c_{furn} + s_{off} p_{fac}) \tag{7}$$

where c_{furn} is the build out cost per office and s_{off} is the size of each office.

References

[1] K. Maxey, *Metal sintering meets industrial needs with the eos m 290 ¿ engineering.com*, https://www.engineering.com/3DPrinting/3DPrintingArticles/ArticleID/7829/Metal-Sintering-Meets-Industrial-Needs-with-the-EOS-M-290.aspx, (Accessed on 05/06/2020), Jun. 2014.

[2] K. S. Fujita, "Commercial discount rate estimation for efficiency standards analysis," 2016.

[3] Haynes International, *Haynes 282 alloy*, (Accessed on 04/29/2020), 2019.

[4] D. M. Dietrich, M. Kenworthy, and E. A. Cudney, *Additive Manufacturing Change Management: Best Practices*. CRC Press, 2019.

[5] EOS GmbH, *Technical data - eos m 290*, https://www.eos.info/en/additive-manufacturing/3d-printing-metal/eos-metal-systems/eos-m-290, (Accessed on 05/05/2020), Jan. 2019.

[6] NextManufacturing Carnegie Mellon University, *Details and cost*, https://engineering.cmu.edu/next/facilities/details-cost.html, (Accessed on 05/07/2020).

[7] EOS GmbH, *Eos m400-4*, https://www.eos.info/en/additive-manufacturing/3d-printing-metal/eos-metal-systems/eos-m-400-4, (Accessed on 12/22/2020).

[8] R. E. Laureijs, J. B. Roca, S. P. Narra, C. Montgomery, J. L. Beuth, and E. R. Fuchs, "Metal additive manufacturing: Cost competitive beyond low volumes," *Journal of Manufacturing Science and Engineering*, vol. 139, no. 8, 2017.

[9] DGI Supply, *Doall dc-400cnc*, https://www.dgisupply.com/product/CMIDC400CNC/;pgid=jkXWMVB7ulZSRphasW29_Dxt0000Mbr-8vXP;sid=Pu3DRFWI27XIRA7k-4gkR0UkXEYNUshmvgJe (Accessed on 12/22/2020).

[10] Lenox Tools, *Guide to Bandsawing*.

[11] ExtrudeHone, *Product data sheet vector*, https://extrudehone.com/wp-content/uploads/2016/04/15001_EH_VECTOR_v06_Final.pdf, (Accessed on 05/07/2020).

[12] US Bureau of Labor Statistics, *Employer costs for employee compensation for the regions – december 2019*, https://www.bls.gov/regions/southwest/news-release/employercostsforemployeecompensation_regions.htm, (Accessed on 05/07/2020), Dec. 2019.

[13] ——, *Engineering technicians, except drafters, all other*, https://www.bls.gov/oes/2017/may/oes173029.htm, (Accessed on 11/11/2020), May 2017.

[14] Statista, *Industrial rents per square foot by type u.s. 2018*, https://www.statista.com/statistics/626555/average-rent-per-square-foot-paid-for-industrial-space-usa-by-type/, (Accessed on 05/05/2020), Nov. 2019.

[15] Global Industrial, *Band saw blades*, https://www.globalindustrial.com/c/metalworking-tools/metalworking-saw-blades/bandsaw-blades, (Accessed on 12/19/2020).

[16] ——, *Metal working fluids*, https://www.globalindustrial.com/c/metalworking-tools/metal-fluids/metalworking-fluids-2, (Accessed on 12/19/2020).

[17] B. Denkena, P. Helmecke, and L. Hülsemeyer, "Energy efficient machining with optimized coolant lubrication flow rates," *Procedia CIRP*, vol. 24, pp. 25–31, 2014.

[18] US Energy Information Administration, "Electric Power Monthly with data for February 2020," Tech. Rep.

[19] US Bureau of Labor Statistics, *Industrial production managers*, https://www.bls.gov/oes/2017/may/oes113051.htm, (Accessed on 12/22/2020), May 2017.

[20] ——, *Quality control inspectors : Occupational outlook handbook: : U.s. bureau of labor statistics*, https://www.bls.gov/ooh/production/quality-control-inspectors.htm, (Accessed on 12/22/2020), Sep. 2020.

[21] W. M. Crain and N. V. Crain, *Federal-regulation-full-study.pdf*, https://www.nam.org/wp-content/uploads/2019/05/Federal-Regulation-Full-Study.pdf, (Accessed on 12/22/2020), Sep. 2014.

[22] Thumbtack, *2020 average small business lawyer cost (with price factors)*, https://www.thumbtack.com/p/small-business-lawyer-cost, (Accessed on 12/22/2020).

[23] Insureon, *Business insurance cost for manufacturers*, https://www.insureon.com/manufacturers-business-insurance/cost, (Accessed on 12/22/2020).

[24] PriceItHere.com, *Compare cost of hr outsourcing in 2020*, https://priceithere.com/hr-outsourcing-prices/, (Accessed on 12/22/2020).

[25] Desert Oasis Commercial Cleaners, *Warehouse cleaning costs 2019*, https://desertoasiscleaners.com/warehouse-cleaning-cost/text\unhbox\voidb@x\bgroup\let\unhbox\voidb@x\setbox\@tempboxa\hbox{A\global\mathchardef\accent@spacefactor\spacefactor}\let\begingroup\let\typeout\protect\begingroup\def\MessageBreak{Ω(Font)}\let\protect\immediate\write\m@ne{LaTeXFontInfo:oninputline106.}\endgroup\endgroup\relax\let\ignorespaces\relax\accent22A\egroup\spacefactor\accent@spacefactor%20one%2Dtime%20heavy%20duty,for%20the%20US%20in%202019., (Accessed on 12/22/2020).

[26] US Bureau of Labor Statistics, *Secretaries and administrative assistants, except legal, medical, and executive*, https://www.bls.gov/oes/current/oes436014.htm, (Accessed on 12/22/2020), May 2019.

[27] S. King, *How much do bookkeeping services for small businesses cost?* https://www.growthforce.com/blog/how-much-bookkeeping-services-cost-small-businesses, (Accessed on 12/22/2020).

[28] CBRE, *2016 north america fit-out cost guide*, https://www.cbre.us/~/media/files/2017/project%20management/2016%20north%20america%20fit-out%20cost%20guide%20-%20occupier%20projects.pdf, (Accessed on 12/22/2020).

[29] IRS, *Publication 946 (2019), how to depreciate property — internal revenue service*, https://www.irs.gov/publications/p946, (Accessed on 12/22/2020).

[30] Valley Box Co, *How much should my packaging cost*, https://www.valleybox.com/hubfs/docs/How-Much-Should-My-Packaging-Cost.pdf, (Accessed on 12/22/2020).

[31] Avasant Research, *It spending as a percentage of revenue by industry, company size, and region*, https://www.computereconomics.com/article.cfm?id=2626, (Accessed on 12/22/2020).

[32] B. Beam-Mellinger, *The average cost per month for office supplies*, https://smallbusiness.chron.com/average-cost-per-month-office-supplies-12771.html, (Accessed on 12/22/2020), Mar. 2019.

[33] C. Cook and J. Graser, "Military airframe acquisition costs: The effects of lean manufacturing," *RAND MR-1325*, 2001, (Accessed on 12/23/2020).

[34] S. Melito, *Manufacturing overhead costs*, https://www.elastoproxy.com/make-buy-part-1-manufacturing-overhead-costs/, (Accessed on 12/23/2020), Jul. 2014.